Alternating Copolymers of Butadiene and Propylene: Properties and Characterization*

W. WIEDER, † H. KROEMER, and J. WITTE, *Bayer AG, Central Research and Development, 5090 Leverkusen, West Germany*

Synopsis

Alternating copolymers of butadiene and propylene (BPR) made by a solution polymerization technique with a modified catalyst of the Furukawa type have highly regular structures. The constitutional repeating unit consists of one propylene and one 1,4-*trans*-butadiene unit. No chain imperfections were detected, except for ≦2% 1,4-*cis*-butadiene units. The configurations of the chiral tertiary carbon atoms in the propylene units could not be directly determined by spectroscopic methods. The intrinsic viscosities of the samples studied lie between 1.1 and 1.8 dL/g. The high molecular weight fractions ($M > 2 \times 10^5$) show long-chain branching. Crystallization effects, namely, a decrease in specific volume with time, and melting are observed after annealing unoriented samples at temperatures between −30 and −50°C. X-ray diffraction shows that the structure of the ordered phase depends on polymerization conditions, varying between a liquid crystal-like close packing of parallel chain segments and imperfect crystalline, three-dimensionally periodic arrangements of chains. Both in the noncrystalline and crystalline ordered phases, the molecules are arranged in layers with a spacing of 0.47 nm. The crystalline chains have nonplanar and not fully extended conformations with a repeat distance of 0.72 nm. The rate of crystallization and the relative decrease in volume (≦1.3%) are small compared to stereoregular polymers like natural rubber and high-cis polybutadiene. In crosslinked specimens, stretched 1:6 to 1:10, the crystalline or liquid crystal-like structure persists up to +60°C. The imperfect nature of the crystallization of BPR is caused by stereoisomerism of the chiral carbon atoms. The chains are probably composed of short tactic sequences separated by atactic arrangements.

INTRODUCTION

Alternating copolymers of butadiene and propylene (BPR, butadiene propylene rubber) with the idealized chain structure

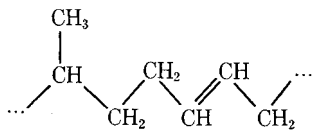

have been known since 1969.[1] Although these interesting copolymers show good processibility, aging characteristics, low-temperature flexibility, resilience, tensile strength, and abrasion resistance,[2–7] they have not yet gained commercial importance. This is probably due to inconvenient reaction conditions and poor catalyst activities in the original polymerization procedure. An improved catalyst for the production of BPR has recently been disclosed.[8] The structural features of the homogeneous vanadium catalyst system used in the latter process were discussed in a preceding article.[9] The polymer obtained by this method

* In memory of Professor Dr. Otto Bayer (4 November 1902–1 August 1982).

† Present address: Bayer Elastomers, B.P. 41, 76170 Lillebonne, France.

Journal of Applied Polymer Science, Vol. 27, 3639–3649 (1982)

CCC 0021-8995/82/103639-11$02.10

has a regular chain structure consisting of a nearly perfectly alternating sequence of 1,4-*trans*-butadiene and propylene units. The molecular weights are sufficiently high so that these polymers can be processed by the usual methods of rubber technology. Some structural characteristics and properties of BPR samples produced by this polymerization process are reported in the present communication.

EXPERIMENTAL

The preparation of the catalyst and the polymerization procedure have recently been described.[8] A number of samples designated as A, B, . . . K, synthesized by use of different catalysts and/or solvents of differing polarities (Table I), were investigated with various techniques.

The limiting viscosity numbers $[\eta]$ were obtained by capillary viscometry. A typical sample was fractionated by precipitation from dilute solution using the system toluene/methanol. The fractions were characterized by intrinsic viscosity measurements, conventional light scattering, and in some cases by 360 MHz proton magnetic resonance spectroscopy (in C_6D_6 solution). The butadiene-to-propylene ratio was determined by evaluation of ^{1}H-NMR spectra. Molecular weight distributions as well as long-chain branching parameters were calculated from the results of GPC (gel permeation chromatography)–$[\eta]$ coupling experiments.[10] The microstructure of the chains was determined by 90.5 MHz proton noise decoupled natural abundance ^{13}C-FT-NMR spectroscopy using a CCl_4/$CDCl_3$ mixture (1 : 1) as solvent.

Dilatometric crystallization data were obtained at −30 and −37°C after keeping the samples 1 h at +60°C in order to destroy athermal nuclei. Glass dilatometers with mercury as immersion liquid were used.

DSC curves were measured on samples which had first been crystallized at

TABLE I
Synthesis Conditions of BPR Samples[a]

Sample	Solvent	$VO(OR)_2Cl$, R =	Conversion, %	$[\eta]$ (toluene, 25°C), dL/g
A	*n*-Hexane	Neopentyl	80	1.72
B	*n*-Hexane	2,2-Dimethyloctyl	53	1.55
C	Methylene chloride	Neopentyl	32	1.57
D	*n*-Hexane	(−)-(1R)Menthyl[b]	58	1.63
E	Toluene	Neopentyl	80	1.74
F	*n*-Hexane	Neopentyl[c]	22	1.68
G	*n*-Hexane	(±)-2-Methylbutyl	25	1.14
H	*n*-Hexane	(−)-2-Methylbutyl	36	1.82
I	*n*-Hexane	Neopentyl[d]	80	2.10
K	*n*-Hexane	Neopentyl[e]	80	0.81

[a] Polymerization conditions: molar ratio butadiene/propylene = 1 : 1; monomer concentration, 30 wt %; 0.5 mmol $VO(OR)_2Cl$ phm; 5 mmol i-Bu_3Al phm; reaction temperature, −50°C; reaction time, 3 h.

[b] $VO(OR_1OR_2)Cl$: R_1 = neopentyl; R_2 = (−)-(1R)menthyl.

[c] Catalyst preformed at −70°C.

[d] High-molecular-weight fraction of sample A.

[e] Reaction temperature −20°C.

TABLE II
Properties of BPR Fractions[a]

Fraction no.	Weight %	$[\eta]$ (THF, 25°C), dL/g	Butadiene, mol %[b]	$M_w \times 10^{-5}$ [c]
1	12.4	1.31	49.5 ± 0.8	
2	13.1	1.16		1.13
3	22.2	0.95		
4	17.7	0.69		0.44
5	14.0	0.50	49.5 ± 0.5	0.24
6	20.6			

[a] Obtained by precipitation fractionation of sample K (toluene/methanol).
[b] 360 MHz proton resonance spectroscopy.
[c] Light scattering.

constant temperature in the DSC instrument and subsequently cooled rapidly below the glass transition temperature T_g so that no further crystallization could take place.

X-ray diffraction patterns of unoriented samples were recorded at room temperature and at −45°C by photographic techniques and counter diffractometry. Crosslinked sheets were made by mixing the polymer in *n*-hexane solution with 1–2.5 wt % dilauroyl peroxide and keeping the mixture 1 h at 110°C in a nitrogen atmosphere after evaporation of the solvent. X-ray diffraction patterns of crosslinked stretched sheets with extension ratios between 1:3 and 1:10 were measured at temperatures between −45 and +70°C with photographic and counter techniques using Ni-filtered Cu K_α radiation.

RESULTS

Molecular Structure

Synthesis conditions and molecular structure data are shown in Tables I and II. The intrinsic viscosities are in most cases above 1.5 dL/g. The molecular weight distributions are comparatively broad (Fig. 1, Table II).

Figure 2 shows the $[\eta]$–M relationship of a typical BPR sample. Long-chain branching starts at a molecular weight M of about 2×10^5 and increases with rising values of M. Similar results were obtained by preparative fractionation and light scattering of the fractions of another sample (Table II).

Table II shows that the chemical composition does not depend on the molecular weight and corresponds exactly, within the limits of experimental error, to that of an ideal alternating copolymer. Not even trace amounts of butadiene homopolymer could be detected. Carbon 13-NMR spectroscopy indicates a nearly perfectly alternating chain structure composed of propylene and 1,4-*trans*-butadiene units. The BPR molecules contain a small percentage (≤2%) of 1,4-*cis*-butadiene units. Other chain irregularities, e.g., butadiene or propylene sequences or head-to-head linkages, do not occur according to 90.5 MHz ^{13}C-NMR. The stereoregularity of the chiral tertiary carbon atoms cannot be determined by 25 MHz ^{13}C-NMR since the distance between consecutive chiral

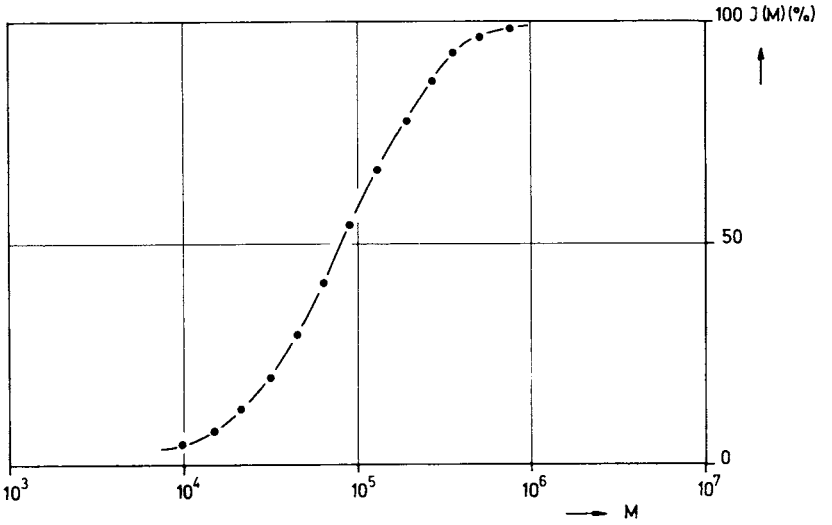

Fig. 1. Cumulative molecular weight distribution of polymer B, obtained by GPC-[η] coupling measurements. Molecular weight averages $M_n = 45 \times 10^3$, $M_w = 160 \times 10^3$.

atoms is too large.[11] The present study using 90.5 MHz ^{13}C-NMR did not furnish evidence for the existence of different linkage dyads (meso and racemic). If there were several types of dyads and triads, additional lines or at least line broadenings would be expected. The broadening should in this case be different for the various signals. However, all lines had nearly equal widths and could be assigned without taking into account stereoisomerism at the tertiary carbon atom. The concentration of racemic dyads should therefore be low (probably less than 20%).

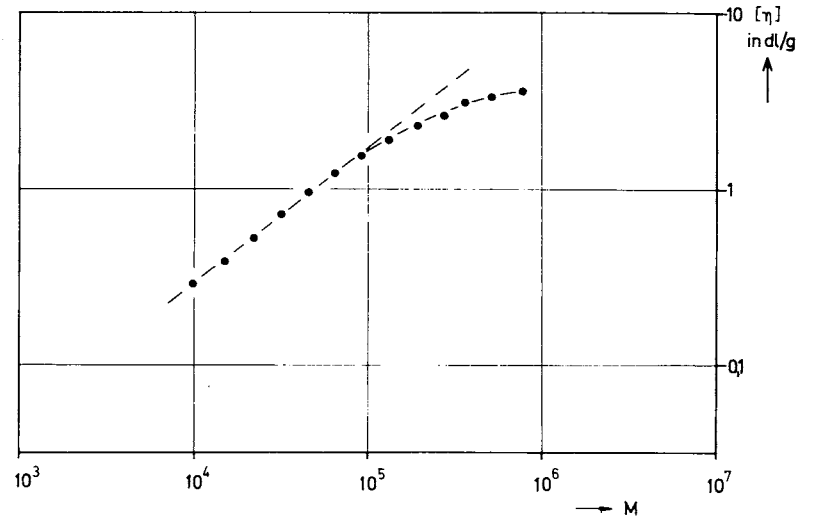

Fig. 2. [η]-M Relationship of polymer B in chloroform at 25°C, obtained by GPC-[η] coupling.

Solid-State Properties and Phase Transitions

The glass transition temperature T_g does not depend appreciably on the polymerization conditions. DSC measurements yielded the value $T_g = -77°C$ for all products studied.

Dilatometry and DSC indicate that BPR is able to crystallize in the isotropic state at sufficiently low temperatures (Table III). (The term "crystallization" is used here for simplicity, although it is shown below that the ordered and dense phases are not in all cases strictly crystalline.) The effects observed, e.g., the change in specific volume and the melting enthalpy, are significantly smaller than in the case of high-cis BR or NR. Likewise, the rates of crystallization are comparatively low. The data of Tables I and III reveal that both the rate of crystallization and the maximum attainable crystallinity depend on the type of catalyst and on the solvent used.

Figure 3 shows a typical crystallization curve obtained by dilatometry. The crystallization mechanism is complex and comprises at least two different processes, a primary and a (much slower) secondary crystallization. The separation of the overall crystallization into these elementary processes is somewhat arbitrary and depends on the theoretical concepts used. However, the half-time τ of the primary process is not much influenced by the way in which this separation is carried out.

An Avrami plot[12] of the primary process (Fig. 4) shows that the Avrami exponent is nearly equal to 3.0 in the initial stage up to times $t \approx \tau$ but becomes smaller at longer times. This means that primary crystallization is initiated at

TABLE III
Thermal Properties of BPR Samples[a]

Sample	T_{cr}, °C	Technique	τ, h	ΔV_p, cm³/100 g	ΔV_{tot}, cm³/100 g	ΔH_m, J/g	T_m, °C
A	−37	DIL	14.5	1.01	1.13		
	−45 (6 h)	DSC	10			16.4	−25
B	−37	DIL	4.3	0.98	1.20		
C	−30	DIL	49	0.48	0.72		
	−37	DIL	3.3	1.09	1.22		
	−37	DSC	3			10.1	−20
	−40 (1 h)	DSC				2.7	−21.5
	−40 (3 h)	DSC	≈2			18.6	−21
	−45 (5 h)	DSC				0.0	
	−45 (1 h)	DSC				4.4	−22.5
	−45 (2 h)	DSC				13.5	−22.5
	−45 (3 h)	DSC				19.8	−22.5
	−45 (6 h)		1.6			20.0	−22
	−50 (1 h)	DSC				0.8	−24
	−50 (3 h)	DSC	≈2–3			18.3	−24.5
D	−37	DIL	12	0.80	0.92		
E	−37	DIL	76	0.45	0.61		
F	−37	DIL	3.7	0.90	1.14		
G	−37	DIL	22	0.63			
	−45 (3 h)	DSC				6.6	−24
H	−37	DIL	15.5	0.55	0.62		

[a] T_{cr}: temperature of crystallization; τ: half-time of primary crystallization; ΔV_p, ΔV_{tot}: decrease in specific volume due to primary and total crystallization process, respectively; ΔH_m: enthalpy of melting; DSC: differential scanning calorimetry; DIL: dilatometry.

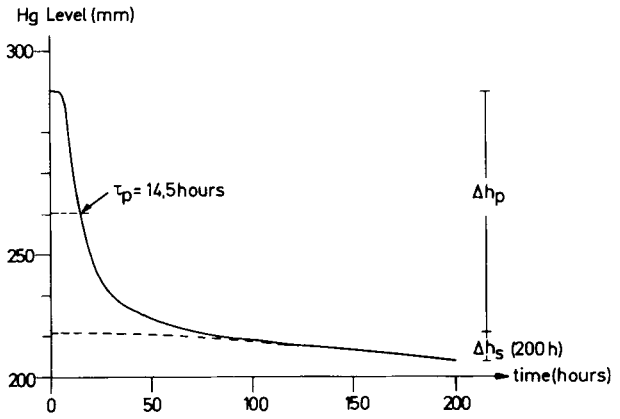

Fig. 3. Dilatometric crystallization curve of polymer A at −37°C. τ_p: Half-time of primary crystallization; Δh_p, Δh_s: changes in mercury level due to primary and secondary crystallization processes, respectively.

the same time $t \approx 0$ by a constant number of preexisting nuclei and proceeds via three-dimensional, probably spherulitic, growth. However, the mechanism of primary crystallization changes at $t > \tau$, and this cannot be described by simple Avrami kinetics. Such effects are often observed in the crystallization of polymers.[13,14] Secondary crystallization proceeds much more slowly and was often not yet completed when the experiment had to be terminated.

Thermoanalytical data are compiled in Table III.

Figure 5 shows a typical crystallization curve obtained by DSC. The melting points T_m given in Table III differ from the equilibrium melting point T_m^0, which is normally not directly measurable. It is possible to estimate T_m^0 by a well-known method[15] involving a plot of T_m vs. T_{cr}, where T_{cr} is the crystallization temperature. Although the application of this method is problematic in the case of melt-crystallized polymers, it yields at least approximate values. $T_m^0 \approx -10$°C is thus obtained for polymer C from the data in Table III.

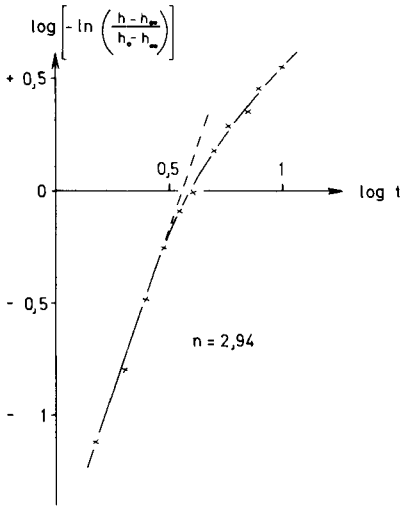

Fig. 4. Avrami plot of the primary crystallization of polymer A at −37°C. h, h_0, h_∞: Instantaneous, initial, and final mercury levels; t: time in hours.

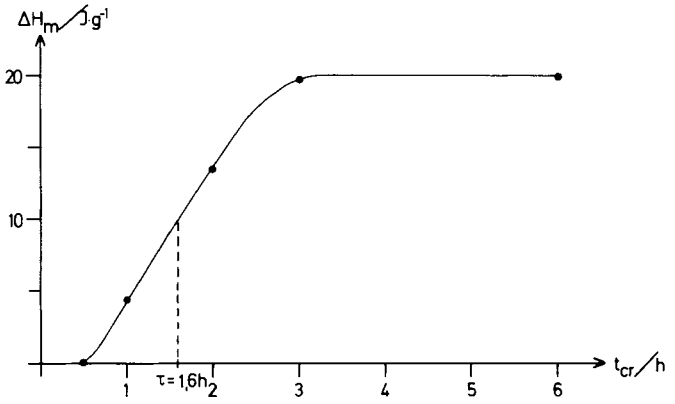

Fig. 5. Crystallization of polymer C at −45°C. Melting enthalpy ΔH_m measured by DSC after crystallization and cooling below T_g in the instrument.

X-ray diffraction (Table IV) supplies information on the spatial arrangement of the chains. At room temperature, isotropic samples show only a broad halo near 0.49 nm (Fig. 6), which is to be expected since they are completely amorphous under these conditions. Diffraction patterns taken at −45°C, after sufficiently long annealing times, exhibit in addition a sharp reflection in the vicinity of the halo (Fig. 7). Further crystalline reflections were not observed. Crosslinked and stretched specimens with extension ratios of 1:6 to 1:10 give X-ray diffraction patterns indicating a high degree of crystal and molecular orientation (Fig. 8). A sharp crystalline reflection appears in these patterns as a small intense spot on the equator. Figure 9 shows an equator scan, taken with a counter diffractometer, of a stretched crosslinked sample at 25°C. The width of the crystalline peak superimposed on the halo corresponds to an apparent crystal size of about 9 nm. The sharp equator reflection is observed up to temperatures of +60°C, thus showing that strain-induced crystallization persists even 70° above the equilibrium melting point.

TABLE IV
X-Ray Diffraction of Oriented Semicrystalline BPR[a]

Layer line	ξ[b]	ζ[b]	I[c]	hkl[d]	d[e]	d_{calc}[e]
0	0.330	0	v st	200	0.467	0.467
0	0.464	0	v w	130	0.332	0.333
0	≈0.52	0	v w	310	≈0.300	0.304
0	0.578	0	w	040	0.267	0.267
0	0.666	0	v w	330	0.232	0.234
				400		0.233
				240		0.232
1	0.167	0.214	w	101	0.568	0.568
2	0	0.427	w	002	0.361	0.361
3	≈0.17	≈0.65	w	103	≈0.23	0.233

[a] Crosslinked sample of polymer I (extension ratio 1:10).

[b] Coordinates of reflections in reciprocal space in units of $1/\lambda$ (ξ perpendicular, ζ parallel to the stretching direction; λ = X-ray wavelength).

[c] Relative intensity (v st = very strong; w = weak; v w = very weak).

[d] Miller indices (orthorhombic cell; see text).

[e] Observed and calculated net plane spacings in nanometers (1 nm = 10 Å).

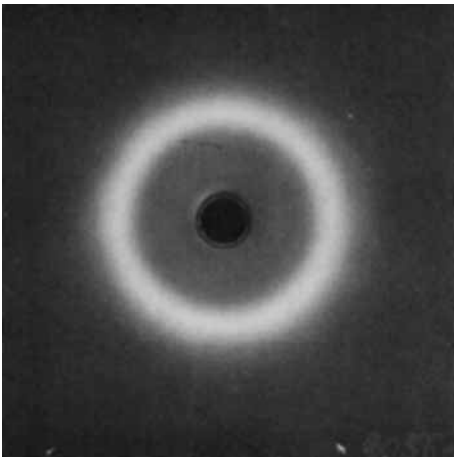

Fig. 6. X-ray diffraction pattern of unoriented BPR at room temperature. Polymer C, Ni-filtered Cu Kα radiation, flat film photograph.

The X-ray diffraction patterns of some crosslinked and highly stretched samples (e.g., sample I) show, in addition to the very strong equatorial reflection at 0.467 nm, a few diffuse and weak reflection spots on the equator and on the first layer lines (Table IV).

The X-ray data can be interpreted as follows: The amorphous halo is due to intermolecular diffraction by a disordered close packing of very short parallel chain segments. On account of the bulkiness of the methyl side groups, the short-range order of the chain segments in the amorphous phase is probably less regular than in linear polymers without side groups.

After crystallization, most samples show only one strong and rather narrow equatorial reflection. In these cases, the crystals are not three-dimensionally periodic and hence must be regarded as liquid crystal-like or paracrystalline arrangements of close-packed chain segments. A comparison with the diffraction

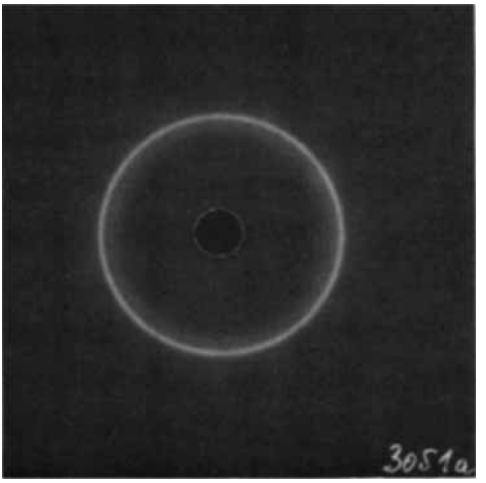

Fig. 7. X-ray diffraction pattern of unoriented polymer C at −45°C. After crystallization time of 3 h.

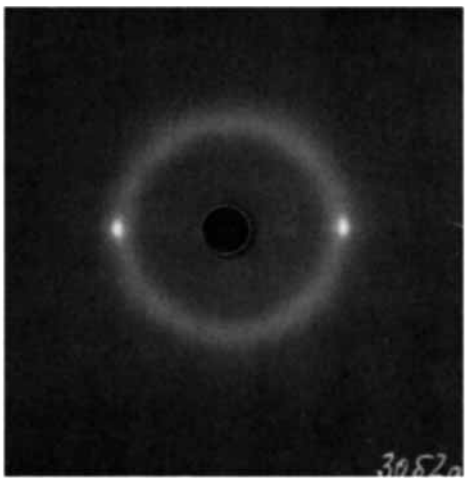

Fig. 8. X-ray diffraction pattern of a crosslinked specimen, stretched 1:10, of polymer C at room temperature.

pattern of a crystalline sample like sample I shows that the molecules in the ordered noncrystalline phase are probably arranged in layers with the same spacing, about 0.47 nm, as in the crystalline phase.

Although the crystalline samples show only a small number of diffuse reflections (Table IV), it is nevertheless possible to draw some conclusions on the crystal structure. The identity period in the chain direction can be calculated from the spacing of layer lines as $c = 0.72$ nm. Since the repeat distance of a fully extended planar all-trans chain would be about 0.755 nm, the crystalline chains must be shortened by rotations about single bonds so that they are nonplanar. The unit cell is probably orthorhombic or monoclinic (with the unique axis along the chain direction) because a reflection is observed exactly at the meridian in the second layer line. The reflections cannot be indexed with certainty, but a

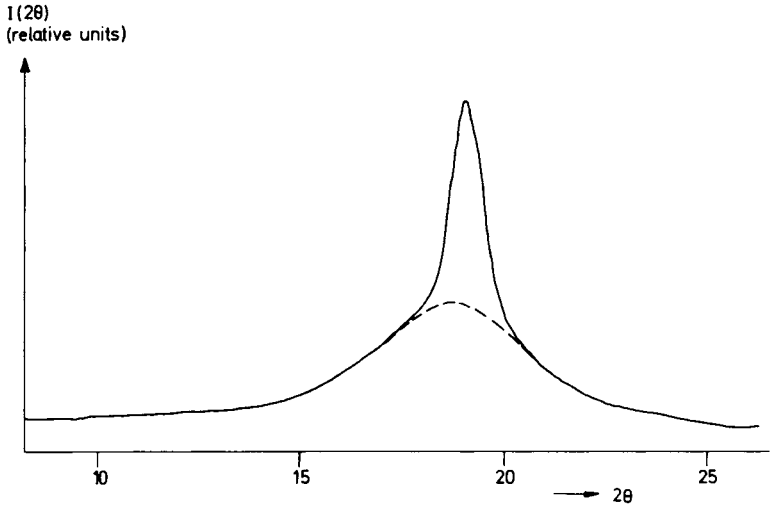

Fig. 9. X-ray diffraction curve of an oriented crosslinked polymer. Equatorial scan, 30°C, sample C, stretched 1:10. Ni filtered Cu K_α radiation, scintillation counter, pulse height discrimination.

tentative assignment assuming an orthorhombic unit cell with $a = 0.933$ nm, $b = 1.068$ nm, and $c = 0.721$ nm fits the observed reflections and yields a reasonable crystal density $\rho_c = 0.89$ g/cm^3. This value agrees with the crystal density estimated from the amorphous density, $\rho_a = 0.871$ g/cm^3 at 25°C, in combination with the observed relative decrease in specific volume during crystallization ($\leqq 1.3\%$). The very high intensity of the first equatorial reflection shows that the crystal structure is essentially built up of layers of molecules with a spacing $a/2 = 0.467$ nm. If the proposed unit cell can be confirmed by further experimental data, the crystal structure of BPR is similar to that of β-guttapercha determined by Bunn.[16]

CONCLUSION

Alternating copolymers of butadiene and propylene possess a very regular constitution without chain imperfections such as head-to-head linkages, butadiene or propylene sequences, etc. The only imperfections that could be detected were small amounts (less than 2%) of 1,4-*cis*-butadiene units.

In view of this regular structure, one would expect BPR to crystallize as well as comparable elastomers, e.g., polyisoprene, if the structure of BPR were stereoregular, i.e., isotactic. Experimental observations do not agree with these expectations:

(1) Crystallinities and crystallization rates of BPR samples are generally much lower than for high-cis polybutadiene or natural rubber.

(2) The crystallization tendencies of different samples depend on the polymerization conditions; polar solvents lead to polymers with higher crystallinity (samples A, C, and E).

(3) Most isotropic samples kept at temperatures below −25°C as well as crosslinked and highly stretched samples at $T \leqq 60$°C contain no crystals with three-dimensional periodicity, but only close-packed arrangements of parallel chains. Disordered crystals were only found in a small number of samples, e.g., sample I.

The different crystallization rates observed are not due to differing concentrations of heterogeneous nuclei (catalyst residues, etc.) or to differing degrees of long-chain branching, because linear fractions of similar molecular weight which contained no heterogeneous impurities showed a strong dependence of the crystallization rate on the type of catalyst or solvent used. Likewise, the imperfect nature of the crystalline phase cannot be explained by the low amount of constitutional imperfections (1,4-*cis*-butadiene units). Since other constitutional chain imperfections could not be detected, the hindered crystallization must be a consequence of sterical irregularity due to the chiral tertiary carbon atoms in the propylene units. Chiral ligands R in the catalyst component $VO(OR)_2Cl$ do not enhance the crystallization rates of the corresponding copolymers (samples D, G, and H).

We conclude that the chains consist of short stereoregular (isotactic) sequences separated by isolated racemic linkages. This assumption accounts for all experimental data in a straightforward manner. For example, differing crystallization properties of products made under different conditions may be explained by variations in the length of stereoblocks. The average block lengths are presently not known, but they can be estimated to comprise about 5 to 20 re-

peating units, depending on the sample. Shorter sequences should be detectable by high-field carbon 13-NMR, whereas appreciable amounts of stereoblocks with more than 20 repeating units would lead to the formation of crystals with three-dimensional periodicity giving characteristic X-ray diffraction patterns, which were only observed in a few cases. Quantitative values for the length distributions of stereoregular sequences may perhaps be accessible by ^{1}H-NMR measurements of suitable selectively deuterated polymers.

The authors are grateful to Dr. M. Hoffmann, Leverkusen, for the viscometric and light scattering data and for part of the dilatometric measurements; to Dr. P. Orth, Leverkusen, for the results of GPC–[η] coupling measurements; and to Dr. D. Wendisch, Leverkusen, for the determination of the microstructure by means of high-field carbon 13 and proton NMR. They would like to express their thanks to Bayer AG for permission to publish this work.

References

1. J. Furukawa, *J. Polym. Sci.*, **7,** 613, 671 (1969).
2. J. Furukawa, *Angew. Makromol. Chem.*, **23,** 189 (1972).
3. J. Furukawa, *Gummi, Asbest, Kunst.*, **10,** 837 (1973).
4. J. Furukawa, *J. Polym. Sci. Symp.*, **48,** 19 (1974).
5. J. Furukawa and E. Kobayashi, *Rubber Chem. Technol.*, **51,** 600 (1978).
6. V. V. Pchelintsev and L. M. Ivanova, *Int. Polym. Sci. Technol.*, **6**(9), T/54 (1979).
7. K. B. Piotrovskii, V. A. Danilova, and A. P. Ivanov, *Int. Polym. Sci. Technol.*, **6**(9), T/56 (1979).
8. J. Witte et al. (to Bayer AG), DE-OS 27 06 118 (1977).
9. W. Wieder and J. Witte, *J. Appl. Polym. Sci.*, **26,** 2503 (1981).
10. W. Scheinert, *Angew. Makromol. Chem.*, **63,** 117 (1977).
11. C. J. Carman, *Macromolecules*, **7,** 789 (1974).
12. M. Avrami, *J. Chem. Phys.*, **7,** 1103 (1939); **8,** 212 (1940); **9,** 177 (1941).
13. H. Krömer, *Naturwissenschaften*, **63,** 328 (1976).
14. M. Hoffmann, H. Krömer, and R. Kuhn, *Polymeranalytik*, Vol. 1, Georg Thieme Verlag, Stuttgart, 1977, p. 96 ff.
15. J. P. Hoffmann and J. J. Weeks, *J. Res. Nat. Bur. Stand.*, **66A,** 13 (1966).
16. C. W. Bunn, *Chemical Crystallography*, Clarendon Press, Oxford, 1946, p. 318 ff.

Received May 21, 1982
Accepted June 1, 1982